Published by IOP Publishing for Sissa Medialab

Received: *March 4, 2026*
Accepted: *April 16, 2026*
Published: *April 30, 2026*

7th International Workshop on New Photon-Detector
Bologna, Italy
3–5 December 2025

Preliminary characterization of the 64-channel MIZAR ASIC for Cherenkov light detection

A. Di Salvo[a,*] **E. Trossarello**[b] **M. Bussi**[b] **F. Reynaud**[a] **M. Abrate**[a] **S. Durandetto**[b] **M. Mignone**[a] **R. Wheadon**[a] **M. Bertaina**[a,b] **S. Garbolino**[a] **and A. Rivetti**[a,c] **on behalf of the JEM-EUSO collaboration**

[a] *Istituto Nazionale di Fisica Nucleare, Section of Torino, Via P. Giuria 1, 10125 Turin, Italy*
[b] *Department of Physics, University of Turin, Via P. Giuria 1, 10125 Turin, Italy*
[c] *Trento Institute for Fundamental Physics and Applications, Via Sommarive 14, 38123 Povo (Trento), Italy*

E-mail: andrea.disalvo@to.infn.it

Abstract: This work presents the implementation and the preliminary tests of the Multi-channel Integrated Zone-sampling Analogue-memory based Readout (MIZAR) ASIC. Developed using commercial 65 nm CMOS technology, the MIZAR ASIC is designed as part of the Cherenkov camera for the POEMMA Balloon with Radio (PBR) mission. The goal of the Cherenkov camera is to detect direct Cherenkov signals produced by Extensive Air Showers (EASs) pointing towards the detector. The broader objective of the PBR mission is the detection of Ultra-High Energy Cosmic Rays (UHECRs) and tau-induced air showers resulting from the interaction of Cosmic Neutrinos with the Earth's crust. In the MIZAR ASIC, a single channel is segmented into 256 acquisition cells and each one includes a capacitor, a Wilkinson Analog-to-Digital Converter (ADC) and a digital memory. This full waveform sampling system operates with an integration time of 5 ns and the data are converted on chip at the same frequency. MIZAR is designed to send out a 64-bit hitmap to use as first-level trigger to recognize patterns of interest. Each channel can be programmed to reduce the sampling window to 32 or 64 cells and the resolution can be set within the interval 8–12 bits. MIZAR was delivered in March 2025 and it has undergone laboratory testing in recent months.

Keywords: Analogue electronic circuits; Digital electronic circuits; Front-end electronics for detector readout; VLSI circuits

*Corresponding author.

https://doi.org/10.1088/1748-0221/21/04/C04092

Contents

1 Introduction 1

2 The MIZAR architecture 1

3 Setup description 2

4 Results 3

4.1 Dark count rate 3

4.2 Single-channel acquisition chain linearity 4

5 Conclusions 5

2026 JINST 21 C04092

1 Introduction

The Multi-channel Integrated Zone-sampling Analogue-memory based Readout (MIZAR) ASIC was developed within the framework of the POEMMA-Balloon-Radio (PBR) mission [1]. PBR is the next generation balloon-borne mission after EUSO-SPB2 [2], a NASA Super Pressure Balloon flown from Wanaka (New Zealand) in May 2023. EUSO-SPB2 payload was based on a fluorescence telescope with a focal plane made of Multi Anode Photo Multiplier Tubes (MAPMTs) for recording the fluorescence emission by EeV-scale EASs and a Cherenkov telescope with a SiPM camera to detect Cherenkov emission from PeV-scale EASs, including those occurrences generated from tau neutrino decays. The PBR shares this design adding a modified Schmidt telescope with a 1-meter primary mirror segmented into four sections. This solution produces two separate focal spots on the sensors via a bifocal optical layout. This approach improves event discrimination due to the differentiation of a single-spot related to direct cosmic ray hits on the focal plane against dual-spot EAS events. In this way, false triggers are reduced and signal fidelity is enhanced. The core of the Cherenkov telescope is based on a high-speed focal plane camera, made of 512 Silicon Photomultiplier (SiPM) pixels (Hamamatsu S13361-3050NE-08 [3]). This camera is optimized for processing nanosecond-scale optical pulses within a 10 ns integration time. An ASIC was developed to perform such kind of fast waveform sampling, digitization on-chip and data readout. This signal processing pipeline enables the accurate reconstruction of the temporal events minimizing the dead time related to the conversion stage.

2 The MIZAR architecture

Figure 1 illustrates the hierarchy of the 64-channel MIZAR chip [4, 5]. Each channel features a front-end analog block that receives the input signal from the SiPM, distributing the processed information across 256 memory cells. The latter combine analog storage with single-slope Wilkinson ADCs to enable parallel digitization at 200 MHz, minimizing system dead time. The ADC resolution is configurable from 8 to 12 bits, allowing lower-resolution operation during background monitoring to reduce overhead. Moreover, the analog memory can be segmented into 32, 64, or 256 cell buffers, supporting multi-buffer acquisition so that an event can be digitized while the system remains ready for subsequent triggers. The chip area is (6×5) mm^2, bounding the power consumption to

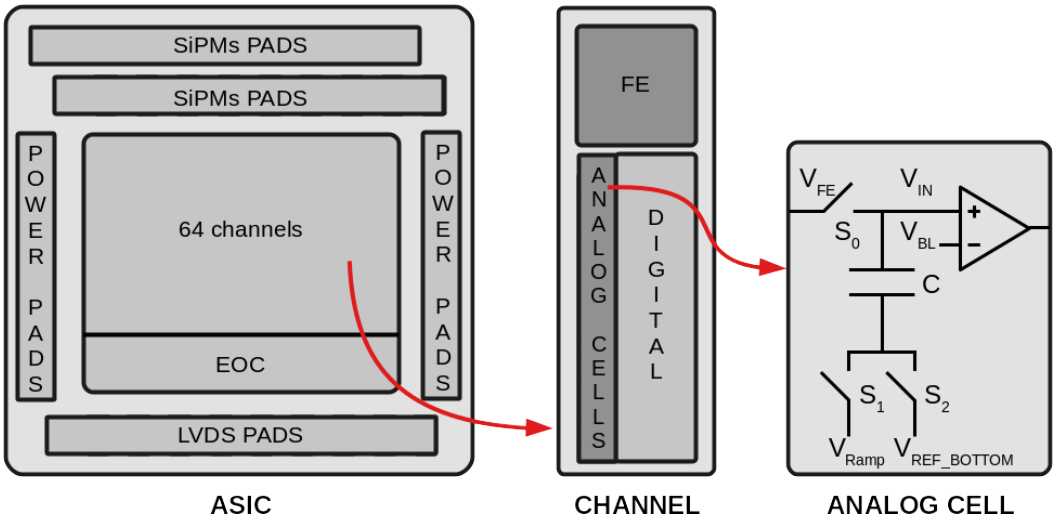

Figure 1. Block diagram of the MIZAR ASIC.

5 mW/channel. Each channel includes high and low adjustable thresholds to detect events concentrated in a single pixel or spanning multiple neighboring pixels. When a signal crosses the low threshold, a programmable validation window starts and if the high threshold is also exceeded within this interval, only the high-threshold trigger is forwarded to the FPGA. Otherwise, the low-threshold trigger is sent. The FPGA analyzes the 64-bit hitmap from each ASIC to determine whether an event qualifies for readout, enabling the digitization. In this way, an efficient data acquisition is ensured for demanding space-based and sub-orbital applications.

3 Setup description

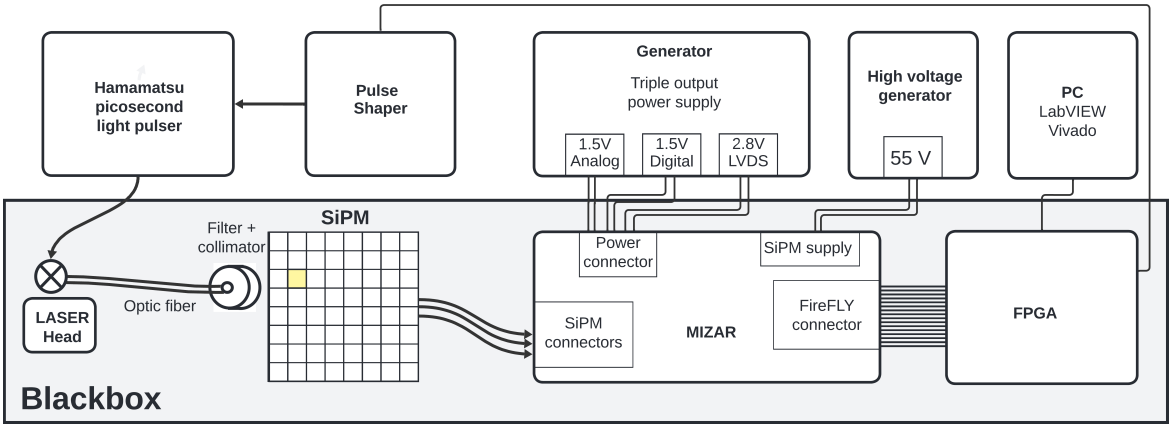

Figure 2. Block diagram of the instrumentation used during the tests.

Figure 2 shows a block representation of the current setup. The MIZAR chip is wire-bonded on the Front-End Board (FEB), which is interfaced with a Genesys 2 FPGA via FireFly cables. The FPGA is connected to a PC running Vivado and LabVIEW, which are used for configuration, control and data acquisition. The FEB is powered by a programmable power supply (Aim-TTi MX100QP S2). The

2026 JINST 21 C04092

SiPM tile is connected directly to the FEB via a pair of high speed coaxial cables. In this configuration, the SiPMs are independently biased at 55 V using a Keithley 2400 SourceMeter operating as a current source. A pulse generator (HP 8012B) is controlled by the FPGA to drive the class 3B LASER light source (Hamamatsu C10196) operating at a waveform of 402 nm. The generated pulses have a width of 40 ns, a period of 290 ns, a maximum amplitude of 10 V and a transition time of 5 ns.

4 Results

4.1 Dark count rate

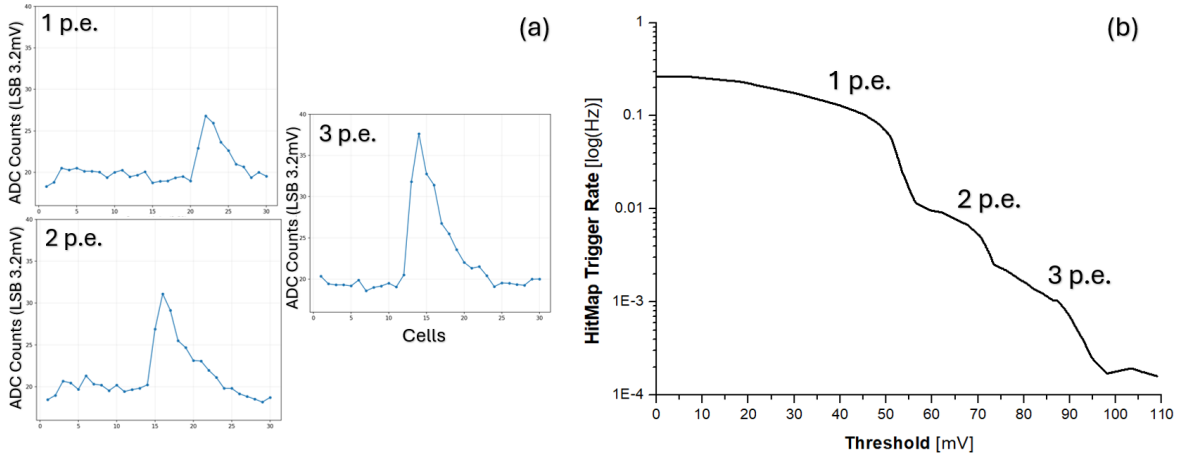

Figure 3. Dark count analysis: a) first three photoelectron peaks, with a 10 ns temporal spacing between samples, and a baseline re-aligned to 20 ADC counts; b) hitmap trigger rate as a function of the low threshold, averaged over the 6-pixel cluster described in the text.

A measurement campaign was conducted to evaluate the single photoelectron sensitivity of the acquisition chain. The I-V curve of the Hamamatsu SiPMs S13361-3050NE-08 was preliminarily measured to determine the breakdown voltage. The device was studied inside the blackbox at the temperature of 21 °C while the reverse bias was scanned using a coarse step of 1 V and a fine step of 250 mV around the breakdown region. The breakdown voltage was extracted from the analysis of the first derivative of the I-V curve resulting in (53.094 ± 0.015)V. The SiPM array was placed inside of an additional light-tight enclosure within the blackbox to prevent any residual light pollution and it was biased at 55 V to replicate the same conditions shown in the datasheet of S13361-3050NE-08. The system performed 100,000 acquisitions for each low threshold value, scanning the [650–1000] mV range in 50 mV steps. For each coarse step, 32 fine steps defined by the Least Significant Bit (LSB) were explored. The measurements were carried out at the temperature of 21 °C setting a buffer depth of 32 analog cells. Data analysis is focused both on hitmap trigger and on waveform samples. Figure 3b shows the trigger rate as a function of the low threshold, averaged over a cluster of 6 pixels operating under equivalent background light conditions, all showing a consistent three-step response. The trend is consistent with the reference curve reported in the datasheet [3]. The raw sampled data were affected by fixed pattern noise, most likely induced by the digital electronics. After removing this noise contribution, the waveform baseline was re-aligned to a common reference level of approximately 20 ADC counts, which remains visible in figure 3a as a residual analog pedestal. Three representative

2026 JINST 21 C04092

waveforms from this corrected dataset are shown in the same figure. To provide a more robust estimator of the peak separation, the photoelectron peaks were located on the peak-area spectrum rather than from the waveform heights, which are sensitive to inter-cell gain variations. The spectrum was smoothed using a Savitzky-Golay filter [6] to suppress statistical fluctuations and local maxima were then identified on the smoothed curve, as shown in figure 4. The four peak positions give spacings of $\Delta\mu = 23.5,\ 25.0,\ 20.5$ and a mean of $\langle\Delta\mu\rangle = 23.0 \pm 1.87$. The uniform spacing confirms that the peaks correspond to successive photoelectron numbers, consistent with the three-step structure observed in the trigger rate plot, indicating single-photoelectron sensitivity.

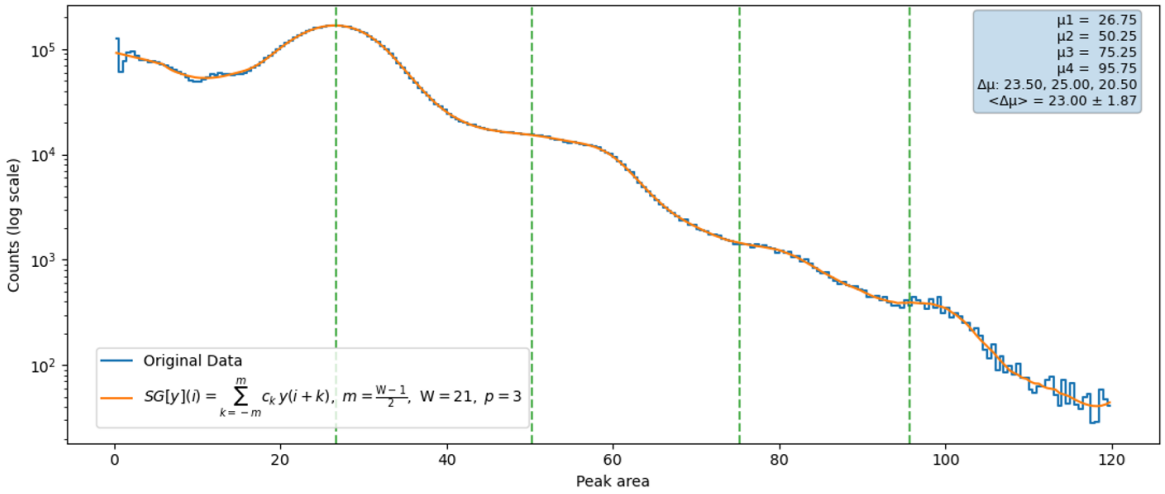

Figure 4. Peak-area spectrum with Savitzky-Golay smoothing. Local maxima identified on the smoothed curve (orange) are marked by dashed vertical lines. The extracted peak positions and spacings are reported in the inset.

4.2 Single-channel acquisition chain linearity

A preliminary study was carried out to verify the linearity of the digitization chain. Since it is not possible to isolate a single ADC within the 256-ADC array of a channel due to the MIZAR architecture, the overall channel response was tested by illuminating the SiPM array with a variable-intensity pulsed laser. The SiPM was placed again inside the black box at 21 °C and biased at 55 V, while the MIZAR ASIC was operating at 8-bit resolution and with a buffer depth of 32 analog cells. The laser linear operating region was preliminarily identified in the [9.5–15.5] a.u. range (potentiometer setting), and it was scanned with a step size of 0.5. For each laser intensity, 100,000 acquisitions were collected and are shown in figure 5. Although it was not possible to scan the full ADC dynamic range without modifying the front-end gain or the Wilkinson ADC ramp slope, the digitization response is found to be linear in the range studied. The uncertainties were initially taken as the standard error of the mean. Since this choice was found to underestimate the measurement uncertainty and the Pearson linear correlation coefficient was acceptable, the RMS residuals was adopted as the *a posteriori* error. Further measurements will be performed to increase the statistic and to extend the study to the unexplored ranges.

2026 JINST 21 C04092

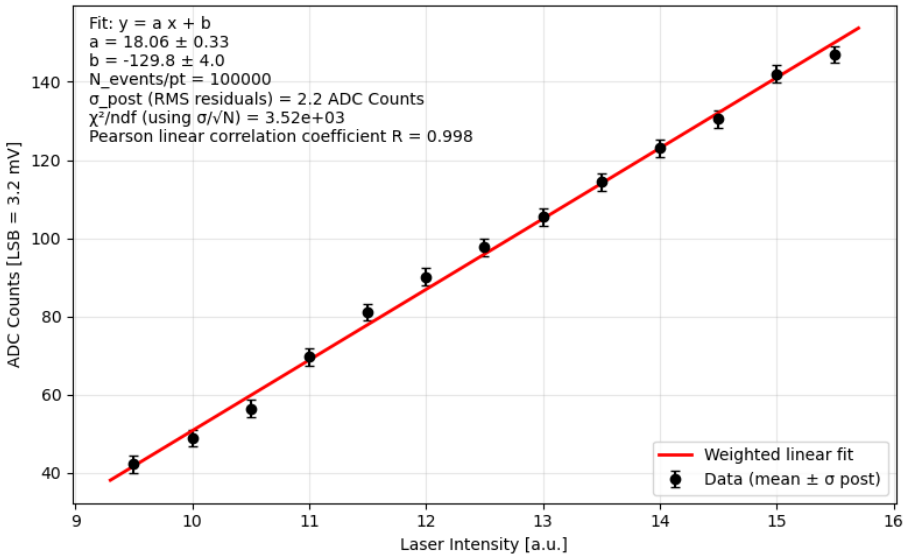

Figure 5. Linear fit of the ADC output versus laser intensity.

5 Conclusions

This paper presents the study of the single-photoelectron sensitivity through the measurement of the dark count rate of the MIZAR ASIC. Moreover, a preliminary single-channel acquisition chain linearity study was conducted using a variable-intensity pulsed laser. For both studies, the device was placed inside a black box at 21 °C and configured with 8-bit ADC resolution and a buffer depth of 32 analog cells, while the SiPM was biased at 55 V. In the dark count rate study, 100,000 acquisitions were collected for each 256 threshold configurations. The data analysis shows consistency between the hitmap trigger rate as a function of threshold and the sampled waveforms plots, suggesting that the device is capable of resolving single photoelectrons. In the linearity study, 100,000 measurements were performed for 13 laser intensities, and the device showed a linear response over a limited portion of the ADC dynamic.

The next steps concern repeating the linearity and sensitivity studies on the 8-MIZAR ASIC flight board, scanning all SiPM pixels using an automated collimation system. The 12-bit resolution and the 400 MHz sampling frequency will also be tested.

Acknowledgments

The MIZAR ASIC described in this article is part of the development performed within the ASI-INFN agreement for EUSO-SPB2 n.2021-8-HH.0 and its amendments. The authors would also like to thank Paolo De Remigis for the support during the setup of the LASER and its safety devices.

2026 JINST 21 C04092

References

[1] M. Battisti, *POEMMA-Balloon with Radio: A balloon-born multi-messenger multi-detector observatory*, *Nucl. Instrum. Meth. A* **1069** (2024) 169819 [arXiv:2409.06753].

[2] J.H. Adams Jr. et al., *The EUSO-SPB2 fluorescence telescope for the detection of Ultra-High Energy Cosmic Rays*, *Astropart. Phys.* **165** (2025) 103046 [arXiv:2406.13673].

[3] Hamamatsu Company, *MPPC (SiPM) array*, https://www.hamamatsu.com/eu/en/product/optical-sensors/mppc/mppc_mppc-array/S13361-3050NE-08.html.

[4] A. Di Salvo et al., *A Configurable 64-Channel ASIC for Cherenkov Radiation Detection from Space*, *Instruments* **7** (2023) 50.

[5] A. Di Salvo et al., *The MIZAR ASIC: 64-channel zone-sampling based ASIC for Cherenkov light detection from sub-orbital and orbital altitudes*, *Nucl. Instrum. Meth. A* **1069** (2024) 169856.

[6] A. Savitzky and M.J.E. Golay, *Smoothing and Differentiation of Data by Simplified Least Squares Procedures*, *Anal. Chem.* **36** (2002) 1627.

2026 JINST 21 C04092